

B. S. T. J. BRIEF

Rain-Induced Differential Attenuation and Differential Phase Shift at Microwave Frequencies

By J. A. MORRISON, M. J. CROSS, and T. S. CHU

(Manuscript received January 15, 1973)

We give calculated results of differential attenuation and differential phase shift caused by rain, based on scattering of a plane electromagnetic wave by horizontally disposed oblate spheroidal raindrops. Two polarizations of the incident wave are considered, as depicted in Fig. 1. The factor $e^{-i\omega t}$ has been suppressed. Subscripts I and II designate electric fields parallel and perpendicular to the plane containing the axis of symmetry of the raindrop and the direction of propagation of the incident wave, respectively. The angle between the direction of propagation and the axis of symmetry is denoted by α . For terrestrial microwave relay systems we take $\alpha = \pi/2$, but for satellite systems other values of α are of interest.

The incident wave induces a transmitted field in the interior of the raindrop, and a scattered field. In the far field the quantities of primary interest are the complex forward scattering functions¹ $S_I(0)$ and $S_{II}(0)$. For the two polarizations considered, the polarization of the far scattered field is the same as that of the incident wave. However, when oblate raindrops are canted with respect to the vertical, the vertical and horizontal polarizations commonly used in radio communications systems will be neither of the two aforementioned polarizations. Then cross-polarization coupling will occur as a result of the difference between $S_I(0)$ and $S_{II}(0)$.

It is assumed that the ratio of minor to major axis of the oblate spheroidal raindrop depends linearly on the radius \bar{a} (in cm) of the equivolumic spherical drop; specifically $a/b = (1 - \bar{a})$. This relationship is similar to that used by Oguchi.² The Laws and Parsons drop-

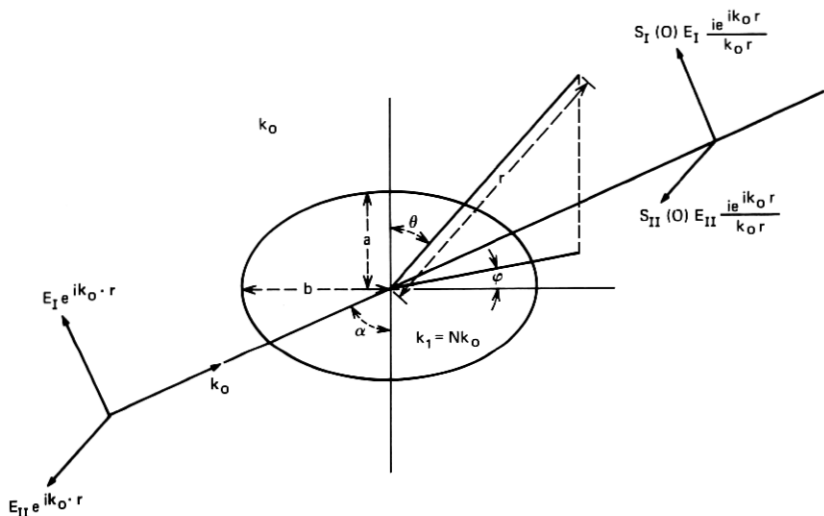


Fig. 1—Two polarizations of the incident wave.

size distribution and Best's raindrop terminal velocity are used.³ Thus, for rain rates up to 150 mm/hour, there are 14 different drop sizes, $\bar{a} = 0.025$ (0.025) 0.35, to be considered. At 20°C, the refractive indices $N = 5.581 + 2.848i$ at 30 GHz and $N = 6.859 + 2.716i$ at 18.1 GHz were obtained from an elaborate fitting equation in a recently published survey⁴ of available measured data. Since the calculations at 4 GHz were made at an earlier date, the value $N = 8.77 + 0.915i$ was taken from the older literature.

Oguchi² has developed a perturbation theory for scattering from slightly eccentric spheroidal raindrops, but the first-order approximation is expected to be inaccurate for the larger raindrops, which have larger eccentricity. Consequently, we have used a matching theory to obtain approximate nonperturbative solutions to the problem. Although the calculations reported on here are for oblate spheroidal raindrops, the procedure may be used for axisymmetric raindrops which are not too nonspherical. Full details of the analytical and numerical procedures, together with tables of the computed values of $S_I(0)$ and $S_{II}(0)$ for each drop size, will be given at a later date, but we outline the approach here.

Spherical coordinates (r, θ, φ) are chosen with polar axis along the axis of symmetry of the raindrop, and origin at the center, as

in Fig. 1. The scattered electric field is expanded in the form $\Sigma\Sigma(a_{mn}\mathbf{M}_{mn} + b_{mn}\mathbf{N}_{mn})$, in terms of solutions of the vector wave equation⁵ satisfying the radiation condition. An analogous expansion is assumed for the transmitted field, in terms of vector wave functions which are finite at the origin. The complex coefficients in the expansions are determined approximately by satisfying the boundary conditions, namely the continuity of the tangential components of the total electric and magnetic fields across the surface of the raindrop, by a fitting procedure. The index m denotes the order of the harmonic in the azimuthal angle φ . The incident field may be expressed as a Fourier series in φ , with coefficients depending on r and θ . Because of this, and the axial symmetry of the raindrop, the problem can be decomposed and the boundary fitting carried out independently for each m .

A large number of points is chosen on the curve which is the intersection of the boundary of the raindrop with the half-plane $\varphi = 0$, $0 \leq \theta \leq \pi$, and the coefficients are determined by requiring the boundary conditions to be satisfied at these points in the least squares sense. The advantage of using least squares fitting rather than collocation (in which the number of fitting points is equal to the number of unknown coefficients, which are then determined by solving a system of simultaneous linear equations) is that the boundary conditions are satisfied more accurately. At least twice as many fitting points as unknown coefficients were used in our calculations. The number of terms required to adequately satisfy the boundary conditions depends on both the frequency and drop size. For example, at 30 GHz it was necessary to take $\max m = 8$ and $\max n = 23$. In order to ensure the accuracy of the leading terms, it is necessary to take more terms in n than are really needed in the calculation of the far-field quantities such as $S_I(0)$ and $S_{II}(0)$. A convergence test was carried out for each drop size, by increasing the upper limit of n in the sums by 2 and by 4. In a number of cases more than half the capacity of a Honeywell 6070 computer was used.

The rain-induced attenuation and phase shift are obtained from the forward scattering functions as follows:¹

$$A_{I,II} = 0.434 \frac{\lambda^2}{\pi} \sum \operatorname{Re} S_{I,II}(0) \mathfrak{R}(\bar{a})^{\text{dB}}/\text{km}$$

$$\Phi_{I,II} = -36 \frac{\lambda^2}{4\pi^2} \sum \operatorname{Im} S_{I,II}(0) \mathfrak{R}(\bar{a})^{\text{deg}}/\text{km}$$

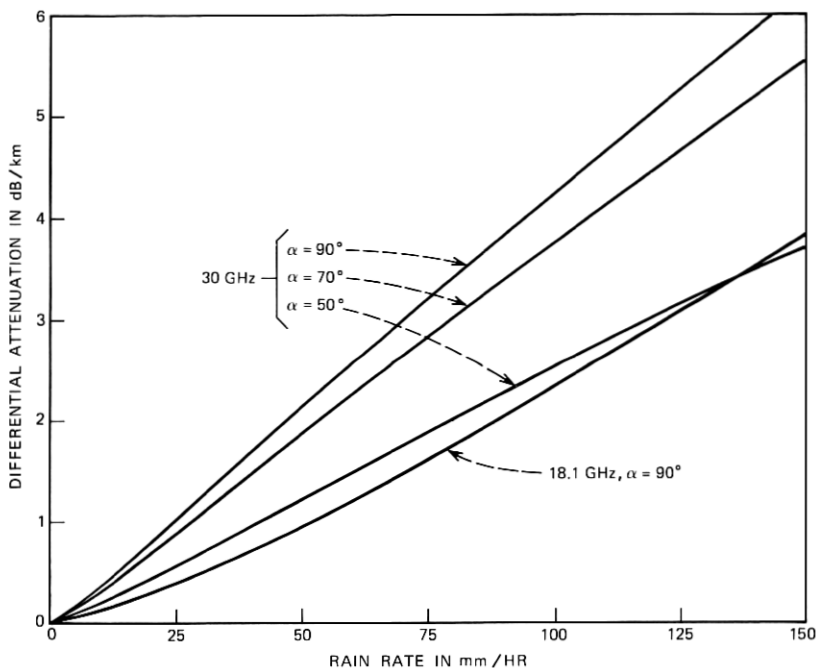


Fig. 2—Rain-induced differential attenuation.

where λ is the wavelength in centimeters, $\mathfrak{N}(\bar{a})$ is the number of raindrops with mean radius \bar{a} per cubic meter, and the summation is taken over all drop sizes. For $\alpha = 90$ degrees, the attenuation and phase shift have been calculated for various rain rates at 4, 18.1, and 30 GHz for polarizations I and II. The cases $\alpha = 50$ degrees and 70 degrees have been calculated at 30 GHz. The differential attenuation $A_{II} - A_I$ and the differential phase shift $\Phi_{II} - \Phi_I$ are summarized in Figs. 2 and 3. Full numerical results will be presented later.

At 4 GHz the differential attenuation is negligibly small (0.036 dB/km at 100 mm/hr), and therefore is not plotted in Fig. 2. However, there is a differential phase shift of 5 deg/km at 100 mm/hr which can induce cross polarization as large as -10 dB over a long path of heavy rain; indeed, such a value was observed experimentally on one occasion by W. T. Barnett.⁶

The calculated differential attenuations for $\alpha = 90$ degrees in Fig. 2 are considerably larger than those obtained by first-order perturbation theory. Taking into account the canting angle distribution,⁷ these

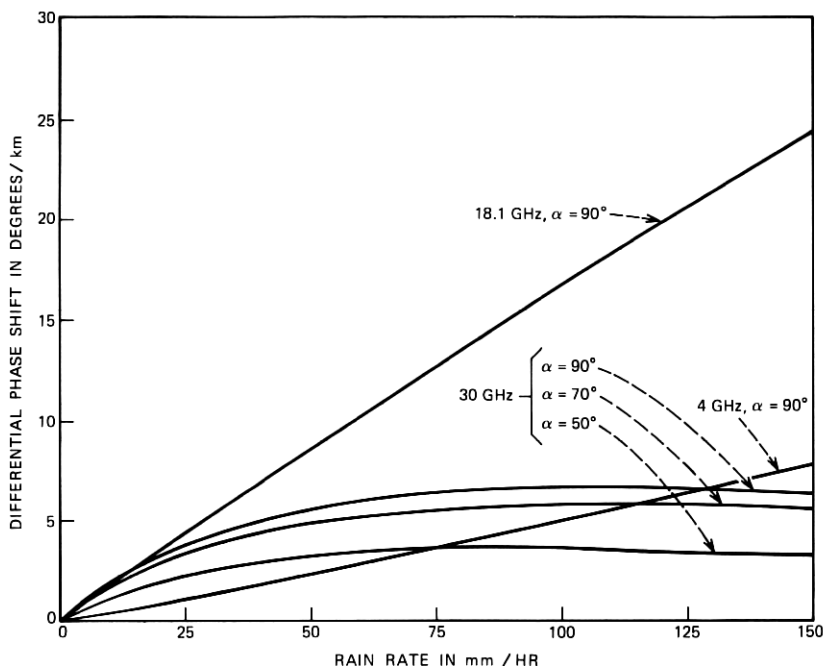


Fig. 3—Rain-induced differential phase shift.

larger values of differential attenuation are needed to explain the measured difference in attenuations for horizontal and vertical polarizations.^{6,8}

At 18.1 GHz the differential attenuation and the differential phase shift will be comparable contributors to rain-induced depolarization. However, the differential phase shift remains small for heavy rain rates at 30 GHz, and hence the differential attenuation will be the dominating cause of rain-induced depolarization at this frequency and presumably also at higher frequencies. When α decreases from 90 degrees, both the differential attenuation and the differential phase shift become smaller as intuitively expected.

The authors are indebted to D. C. Hogg for bringing this problem to their attention, to J. McKenna and N. L. Schryer for suggesting the matching and least squares fitting approaches, and for several helpful discussions in relation to these, to P. A. Businger whose least squares fitting subroutine was incorporated into the main program, to Mary Ann Gatto who took over the burdensome task of running the main

program, to Susan Hoffberg who wrote the program for calculating the first-order approximation for small eccentricities, and to Diane Vitello who performed the summation over the drop size distribution. The authors are particularly indebted to J. McKenna and D. C. Hogg for their continued encouragement throughout the lengthy course of this work.

Note added in proof:

A very recent paper by Oguchi,⁹ in which similar calculations are carried out for $\alpha = \pi/2$ at 19.3 and 34.8 GHz, has come to our attention. He used collocation for the expansions in terms of spherical vector wave functions, and at 34.8 GHz he also used an expansion in terms of spheroidal wave functions.

REFERENCES

1. Van de Hulst, H. C., *Light Scattering by Small Particles*, New York: Wiley, 1957.
2. Oguchi, T., "Attenuation of Electromagnetic Wave Due to Rain with Distorted Raindrops," J. Radio Res. Labs. (Tokyo), Part 1 in 7, No. 33 (September 1960), pp. 467-485; Part 2 in 11, No. 53 (January 1964), pp. 19-44.
3. Kerr, D. E., *Propagation of Short Radio Waves*, New York: McGraw-Hill, 1951.
4. Ray, P. S., "Broadband Complex Refractive Indices of Ice and Water," Appl. Opt., 11, (August 1972), pp. 1836-1844.
5. Stratton, J. A., *Electromagnetic Theory*, New York: McGraw-Hill, 1941.
6. Barnett, W. T., private communication.
7. Saunders, M. J., "Cross Polarization at 18 and 30 GHz Due to Rain," IEEE Trans. Ant. and Prop., AP-19, No. 2 (March 1971), pp. 273-277.
8. Semplak, R. A., "Effect of Oblate Raindrops on Attenuation at 30.9 GHz," Radio Sci., 5, (March 1970), pp. 559-564.
9. Oguchi, T., "Attenuation and Phase Rotation of Radio Waves Due to Rain: Calculations at 19.3 and 34.8 GHz," Radio Sci., 8, (January 1973), pp. 31-38.